A Numerical Investigation on Transport Phenomena in a Nanofluid Under the Transverse Magnetic Field Over a Stretching Plate Associated with Solar Radiation

Shiva Rao and P. N. Deka

Abstract This numerical investigation considers the solar radiation effect on a nanofluid over a stretching plate acted upon by a transverse magnetic field focusing on the stagnation points. Here, linear Roseland approximation is applied for solar radiation. The physical flow problem is modeled using the sets of partial differential equations, which are then transformed into a set of non-linear ordinary differential equations by using the appropriate similarity transformation. We have a new bvp4c solver in the MATLAB platform to solve the equations numerically to investigate the solar radiation effect on various flow parameters associated with MHD nanofluids such as Brownian motion, velocity, temperature and concentration. A comparative analysis is performed for the results with previous studies in some limiting cases to prove the efficiency of the numerical approach. The results have been presented graphically as well as in tabular form to intricate the flow pattern.

Keywords MHD flow · Solar radiation · Stretching plate · Rosseland approximation · Stagnation point · Brownian motion

1 Introduction

Growing energy demand and associated energy crises coupled with environmental issues are now considered with priority across the globe. Attention towards renewable energy has increased as these can replace fossil fuels and reduce the ejection of Green House Gases. Out of different renewable energies like hydro-power from water, geothermal energy, wind energy, biomass from plants, solar energy is one of the cleanest renewables that comes directly from the sun and can be transformed into electricity directly by photoelectric effect and into heat by photo-thermal conversion. Hence, the implementation of solar energy has gained mass attention recently.

Voltaic cells and solar thermal plants are the main gateways to use solar energy and its efficiency can be increased by improving solar energy absorption. The dependence

S. Rao (✉) · P. N. Deka
Dibrugarh University, Dibrugarh, Assam 786004, India
e-mail: shivarao374@gmail.com

S. Banerjee and A. Saha (eds.), *Nonlinear Dynamics and Applications*,
Springer Proceedings in Complexity,
https://doi.org/10.1007/978-3-030-99792-2_39

on fossil fuel can be reduced by using renewable energy which mainly relies on the absorption of solar energy and conversion into thermal energy. However, there is a significant loss of energy in the absorption of sunlight by collecting panels. The weak thermo-physical properties of convectional fluids make it non-viable to construct heat exchangers with greater efficiency [1]. The water-dispersed nano-particles are found to improve the absorption of sunlight [27]. To increase the absorption efficiency different researchers have tested different nano-particles. In recent decades, nanofluids are extensively used in collectors as they elevate greater heat elimination due to their superiority in thermo-physical properties in comparison to traditional fluid [20].

Nowadays, industrial fluids are studied by researchers very intensively. Recently, there has been a great discussion about the parameters behind the heat transfer in nanofluid, despite many studies done already [33]. Nanofluids are made by the suspension of nanoparticles in the base fluid. Choi [5] was the first researcher to discover that the suspended nanoparticles in the base fluid could enhance the thermal conductivity. Lee et al. [19] measured the thermal conductivity of different metal oxides and revealed that both shape and size played an important role in enhancing thermal conductivity of the nanofluid. Nanoparticles not only increase thermal conductivity but also increase the heat transfer capacity by convection [25]. Eastman et al. [7] by their study conclude that the addition of copper nanoparticles with volume fraction less than 1% in ethylene glycol could increase the thermal conductivity up to 40%. Buonigiorno [4] attempted to explain the increase in the thermal conductivity of the nanofluid by pointing out two slip mechanism i.e., Brownian motion and thermophoresis for effective enhancement of thermal conductivity of the base fluid. MHD nanofluid has a great significance in engineering. Buongiorno's model [4] of viscous and incompressible nanofluid flow between a vertical flat plate and a porous medium was investigated by Nield and Kuznetsov [18]. Khan and Pop [16] were the first to investigated the evolution of heat transfer and nanoparticle volume fraction in a nanofluid across a stretching sheet. Rana and Bhargava [28] used the FEM approach to solve Khan and Pop's problem for the nonlinearly stretching sheet. Makinde and Aziz [23] investigated the heat transfer properties in nanofluid flow utilising convective boundary conditions. The convectional flow in a square duct in the presence of a high transverse magnetic field was investigated by Chutia and Deka [6]. Some recent work on MHD nanofluid are presented in Refs. [12, 13, 15, 30].

Thermal radiation on natural convection has become a great importance due to its wide range application is physics and engineering especially in the design of components and equipment, space technology and gas turbine, etc. Unlike conduction and convection, thermal radiation does not need any medium to transmit the heat. These properties make thermal radiation much significant in heat transfer of MHD nanofluid as it reduces the loss of heat. England and Emery [8] investigated the effect of thermal radiation on the natural convective boundary layer flow along vertical plate for absorbing and non-absorbing gases. Kumar et al. [17] presented an idea of the impact of thermal radiation on nanofluid model for flow and heat transfer over an infinite vertical plate under magnetic field and viscous dissipation.

Ali et al. [2] studied the impact on thermal radiation and non-uniform heat flux of the MHD hybrid nanofluid over the stretching cylinder. The effect of hall current which chemical reaction and thermal radiation of a nanofluid flow in a rotating channel was numerically investigated by Lv et al. [22].

Improvement in Solar collector model is one of the major priority for the use of solar energy. Nanofluid is used as a main operating fluid in most of the solar collector nowadays. Javadi et al. [14] have studied the working principle of nanofluid on solar collector in details. Yousefi et al. [35] used Al_2O_3-water nanofluids as an operating fluid in solar collector and draw a very interesting conclusion that the nanofluid based model inceases the efficiency of solar collector by 28.3%. Faizal et al. [9] claim the possibility to make a smaller solar collector, using different nanofluid which produces the same output as the larger one. The action of CuO-water and water in a solar collector was compared by Liu et al. [21]. Sarkar and Kundu [31] studied an unsteady MHD nanofluid near a spinning sphere in the presence of solar radiation. Mushtaq et al. [24] studied the radiation effect of the MHD nanofluid flow in the two-dimensional form through the Runge–Kutta method with an appropriate shooting technique. Ghasemi et al. [10, 11] used the Keller box and Differential quadrature method (DQM) to conduct a numerical analysis of Mushtaq's work under the effects of radiation.

In this study, an investigation is done numerically with the following highlights:

- PDE's are reduced to the sets of ODE's by using similarity transformation.
- MATLAB build-in solver bvp4c is used to solve the ODE's to investigate the non-linear radiative transport phenomena in nanofluid flow under the action of transverse magnetic field under solar radiation.
- This study presents a nanofluid model for a solar collector by considering some thermal effects which can increase its efficiency to much extend.
- The study presents the velocity, temperature and concentration profiles to investigate the effect of solar radiation along with the other MHD flow parameters.
- The validity of the current results is verified by Mushtaq et al. [24]'s previous study.
- Graphical results are discussed in details with physical reasoning to clarify findings.
- The Nusselt number and Sherwood number for various parameters are thoroughly explored.

2 Mathematical Formulation

In the present study, we consider a steady two dimensional flow of a nanofluid under transverse magnetic field over a stretching sheet under the Solar radiation. As shown in Fig. 1 the stretching sheet is placed at y = 0 and the fluid start flowing towards x-axis when the sheet is stretched (force applied) along the same axis. The magnetic field B_o acts perpendicular to the direction of the flow. The stretching velocity along the x-axis is $u_w = ax$ and velocity outside the boundary layer is $u_\infty = bx$.

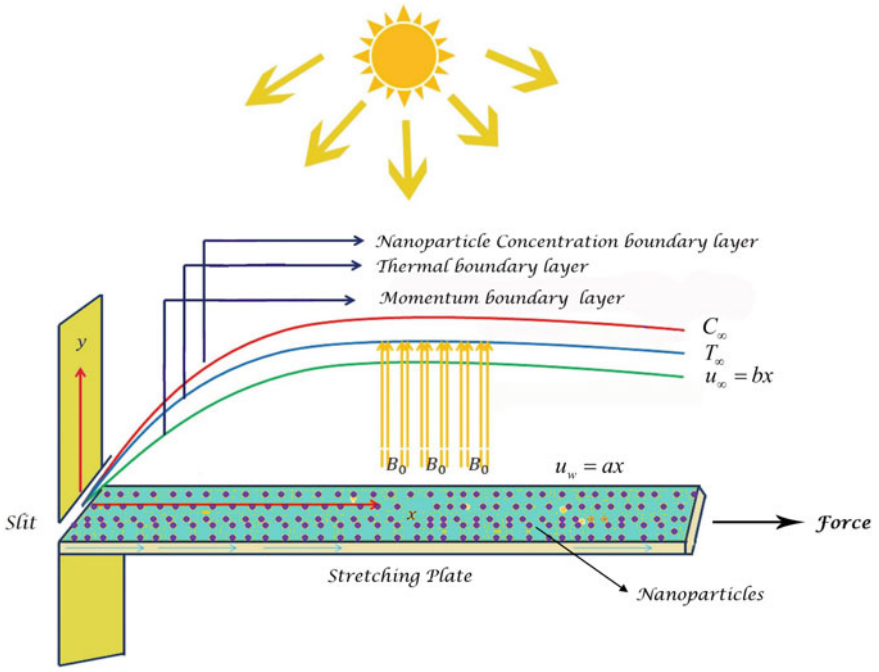

Fig. 1 Schematic diagram of the problem

The system of governing equations (see Refs. [18, 26, 32]) of the flow is given as follows:

$$\frac{\partial u}{\partial x} + \frac{\partial v}{\partial y} = 0 \tag{1}$$

$$u\frac{\partial u}{\partial x} + v\frac{\partial u}{\partial y} = u_\infty \frac{\partial u_\infty}{\partial x} + \nu_f \frac{\partial^2 u}{\partial y^2} - \frac{\sigma_e B_o^2}{\rho_f}(u - u_\infty) \tag{2}$$

$$u\frac{\partial T}{\partial x} + v\frac{\partial T}{\partial y} = \alpha\frac{\partial^2 T}{\partial y^2} + \frac{\nu_f}{C_f}\left(\frac{\partial u}{\partial y}\right)^2 - \frac{1}{(\rho C)_f}\left(\frac{\partial q_r}{\partial y}\right) + \frac{\sigma_e B_o^2}{(\rho C)_f}(u - u_\infty)^2 +$$
$$\tau\left[D_B\frac{\partial T}{\partial y}\frac{\partial C}{\partial y} + \frac{D_T}{T_\infty}\left(\frac{\partial T}{\partial y}\right)^2\right] + \frac{Q_o}{\rho_{f C_p}}(T - T_\infty) \tag{3}$$

$$u\frac{\partial C}{\partial x} + v\frac{\partial C}{\partial y} = D_B\frac{\partial^2 C}{\partial y^2} + \frac{D_t}{T_\infty}\frac{\partial^2 T}{\partial y^2} \tag{4}$$

where u and v are velocity component along the direction of x-axis and y-axis respectively, T is the temperature and C is the nanoparticle concentration, $\nu_f = \frac{\mu_f}{\rho}$ is the kinematic viscosity, σ_e is the electrical conductivity, $\alpha = \frac{\kappa}{(\rho C)_f}$ is the thermal

diffusivity, q_r is the radiation parameter, Q_o is the internal heat generation/absorbtion coefficient, D_B and D_τ are coefficients of Brownian and thermophoretic diffusion parameter respectively. In this case, we consider the Rosseland approximation for radiation heat flux, which is mathematically expressed as (see Refs. [3, 29, 34]):

$$q_r = -\frac{-4\sigma^*}{3k^*}\frac{\partial^4 T}{\partial y} \tag{5}$$

where σ^* and k^* are Stefan-Boltzmann and mean absorption coefficient respectively.

Expanding the Taylor series and neglecting the higher order, we get

$$\mathrm{T}^4 = 4\,\mathrm{T}_\infty^3\,\mathrm{T} - 3\,\mathrm{T}_\infty^4$$

Hence Eqs. (5) becomes-

$$\frac{\partial \mathrm{q_r}}{\partial \mathrm{y}} = \frac{-16\sigma^*}{3\mathrm{k}^*}\,\mathrm{T}_\infty^3\,\frac{\partial^2 \mathrm{T}}{\partial \mathrm{y}^2} \tag{6}$$

The boundary conditions (see Ref. [16]) for the considered problem are:

$$\begin{aligned} &u = u_w(x) = ax,\ v = 0,\\ &-k\frac{\partial T}{\partial y} = h\big(T - T_f\big),\ C = C_w \ \text{ at } \ y = 0.\\ &u \to u_\infty(x) = bx,\ T \to T_\infty,\ C \to C_\infty \text{ as } y \to \infty \end{aligned} \tag{7}$$

The similarity transformation used to make Eqs. (1) to (4) dimensionless are as follows (see Ref. [18]):

$$\begin{aligned} &\eta = \sqrt{\tfrac{a}{\nu_f}}\,y,\ u = axf'(\eta),\ v = -\sqrt{a\nu_f}\,f(\eta),\\ &\theta = \tfrac{T-T_\infty}{T_f-T_\infty},\ \phi = \tfrac{C-C_\infty}{C_w-C_\infty} \end{aligned} \tag{8}$$

The set of PDE's (2) to (4) are transformed by using the set of transformation Eq. (7) to obtain:

$$f'''(\eta) + f(\eta)f''(\eta) - (f'(\eta))^2 + \lambda^2 + M(\lambda - f'(\eta)) = 0 \tag{9}$$

$$\begin{aligned} &\frac{1}{Pr}[1 + (Rd\big(1 + (\theta_w - 1)\theta(\eta)\big)^3]\theta''(\eta) + f(\eta)\theta'(\eta) + A\theta + N_b\theta'(\eta)\phi'(\eta) +\\ &N_t(\theta'(\eta))^2 + E_c(f''(\eta))^2 + ME_c(\lambda - f'(\eta))^2 = 0 \end{aligned} \tag{10}$$

$$\phi''(\eta) + Lef(\eta)\phi(\eta) + \frac{N_t}{N_b}\theta''(\eta) = 0 \tag{11}$$

where $M = \frac{\sigma B_o^2}{\rho_f a}$ is the parameter associated with magnetic field strength, $\lambda = \frac{b}{a}$ is the ratio of rates of free stream velocity to the velocity of the stretching sheet, $Pr = \frac{\nu_f}{\alpha}$ is the Prandtl number, $R_d = \frac{16\sigma^* T_\infty^3}{3kk^*}$ is the Radiation parameter, $\theta_w = \frac{T_f}{T_\infty}$ is the Temperature parameter, $N_b = \frac{\tau D_B (C_w - C_\infty)}{\nu_f}$ is the Brownian motion parameter, $N_t = \frac{\tau D_t (T_w - T_\infty)}{T_\infty \nu_f}$ is the Theromophoresis parameter, $A = \frac{Q_o}{a\rho_f C_p}$ is the heat source and heat sink parameter for $A > 0$ and $A < 0$ respectively, $E_c = \frac{u_w}{C_p(T_w - T_\infty)}$ is the Eckert number and $Le = \frac{\nu_f}{D_B}$ is the Lewis number.

The boundary condition (7) in the dimensionless form are as follows:

$$f(0) = 0,\ f'(0) = 1, \theta'(0) = -\gamma[1 - \theta(0)], \phi(0) = 1$$

$$f'(+\infty) \to \lambda, \theta(+\infty) \to 0, \phi(+\infty) \to 0 \tag{12}$$

where $\gamma = \frac{h}{k\sqrt{\frac{\nu_f}{\alpha}}}$ is the Biot number.

The surface heat flux and mass flux in dimensionless form can be represented as follows:

$$\frac{Nu_x}{\sqrt{Re_x}} = -\left[1 + Rd\theta_w^2\right]\theta'(0) = Nur \tag{13}$$

$$\frac{Sh}{\sqrt{Re_x}} = -\phi'(0) = Shr \tag{14}$$

3 Method of Solutions

The dimensionless ordinary differential Eqs. (9) to (11) along with dimensionless boundary conditions (12) are solved using a MATLAB built-in solver bvp4c package. The equations are converted into the set of first order differntial equations as follows:

$$f = y_1, f' = y_1' = y_2, f'' = y_2' = y_3, \theta = y_4,$$

$$\theta' = y_4' = y_5, \phi = y_6, \phi' = y_6' = y_7$$

$$f''' = y_3' = y_2^2 - y_1 y_3 + \lambda^2 + M(\lambda - y_2) \tag{15}$$

$$\theta'' = y_5' = \frac{-\mathrm{Pr}[y_1 y_5 + A y_4 + N_b y_5 y_7 + N_t y_7^2 + E_c y_3^2 + M E_c (\lambda - y_2)^2]}{1 + Rd(1 - (\theta_w - 1)y_4)^3} \tag{16}$$

$$\phi'' = y_7' = -Ley_1y_7 - \frac{Nt}{Nb}y_5 \tag{17}$$

The boundary conditions are given by:

$$\begin{aligned} &y_1(0) = 0,\ y_2(0) = 1,\ y_5(0) = -\gamma[1 - y_4(0)],\ y_6(0) = 1, \\ &y_2(+\infty) = \lambda,\ y_4(+\infty) = 0,\ y_6(+\infty) = 0 \end{aligned} \tag{18}$$

4 Results and Discussions

Influence of non-dimensional parameter such as Radiation parameter R_d, along with Brownian motion parameter N_b, Thermophoresis parameter N_t, Magnetic field parameter M, Lewis number Le, Biot number γ, Prandtl number Pr and Eckert number E_c on Temperature profile $\theta(\eta)$, Nanoparticle concentration $\phi(\eta)$, reduced Nusselt number and reduced Sherwood number graphically and numerically.

The obtained numerical solutions are compared with those of prior published Mushtaq et al. [24] to justify the correctness of the employed approach. Table 1 illustrates the numerical value of heat and mass transfer, as well as the results reported by [24] in the presence and absence of radiation, which demonstrates great agreement with the results achieved in this investigation.

Table 2 shows the effect of radiation, together with other parameters, on heat and mass transfer as numerical values of $-\theta'(0)$ and $-\phi'(0)$.

Figures 2 and 3 depict the effect of N_t along with R_d on the temperature profile and Nanoparticle concentration profile respectively and it can be observed that the

Table 1 Comparison of values of $-\theta'(0)$ and $-\phi'(0)$ for the various value of N_b with Mushtaq et al. [24]

N_b	R_d	Mushtaq et al. [24]		Present study	
		$-\theta'(0)$	$-\phi'(0)$	$-\theta'(0)$	$-\phi'(0)$
0.1	0	0.078993	2.44780	0.0785	2.4478
	1	0.081387	2.40369	0.0815	2.4061
0.2	0	0.070373	2.43727	0.0704	2.4373
	1	0.078183	2.39810	0.0779	2.4001
0.3	0	0.058202	2.44012	0.0582	2.4401
	1	0.074496	2.39670	0.0735	2.3991
0.4	0	0.040852	2.44673	0.0409	2.4467
	1	0.070375	2.39623	0.0681	2.3970
0.5	0	0.018834	2.45314	0.0189	2.4531
	1	0.065911	2.39605	0.0615	2.3961

Table 2 Value of Nur and Shr for different parameters along with radiation

R_d	N_t	N_b	M	Pr	Le	γ	E_c	$-\theta'(0)$	$-\phi'(0)$
0	0.1	0.1	0.5	5.0	1.0	0.1	0.1	0.0880	0.6586
	0.2							0.0879	0.6211
	0.3							0.0878	0.5847
1	0.1	0.1	0.5	5.0	1.0	0.1	0.1	0.0871	0.6589
	0.2							0.0870	0.6213
	0.3							0.0869	0.5846
0	0.1	0.1	0.5	5.0	1.0	0.1	0.1	0.0880	0.6586
		0.2						0.0650	0.6812
		0.3						0.0847	0.6891
1	0.1	0.1	0.5	5.0	1.0	0.1	0.1	0.0871	0.6589
		0.2						0.0860	0.6801
		0.3						0.0848	0.6874
0	0.1	0.1	0.5	5.0	1.0	0.1	0.1	0.0880	0.6586
			1.0					0.0866	0.6599
			1.5					0.0853	0.6616
1	0.1	0.1	0.5	5.0	1.0	0.1	0.1	0.0871	0.6587
			1.0					0.0860	0.6580
			1.5					0.0850	0.6577
0	0.1	0.1	0.5	5.0	1.0	0.1	0.1	0.0880	0.6586
				7.0				0.0881	0.6602
				9.0				0.0880	0.6622
1	0.1	0.1	0.5	5.0	1.0	0.1	0.1	0.0871	0.6589
				7.0				0.0877	0.6581
				9.0				0.0880	0.6583
0	0.1	0.1	0.5	5.0	1.0	0.1	0.1	0.0880	0.6586
					4.0			0.0870	1.4480
					7.0			0.0865	1.9696
1	0.1	0.1	0.5	5.0	1.0	0.1	0.1	0.0871	0.6589
					4.0			0.0865	1.4408
					7.0			0.0863	1.9586
0	0.1	0.1	0.5	5.0	1.0	0.1	0.1	0.0880	0.6586
						0.2		0.1651	0.6061
						0.3		0.2329	0.5601
1	0.1	0.1	0.5	5.0	1.0	0.1	0.1	0.0871	0.6589
						0.2		0.1598	0.6147
						0.3		0.2213	0.5776

(continued)

Table 2 (continued)

R_d	N_t	N_b	M	Pr	Le	γ	E_c	$-\theta'(0)$	$-\phi'(0)$
0	0.1	0.1	0.5	5.0	1.0	0.1	0.1	0.0880	0.6586
							0.2	0.0826	0.6844
							0.3	0.0771	0.7103
1	0.1	0.1	0.5	5.0	1.0	0.1	0.1	0.0871	0.6589
							0.2	0.0830	0.6764
							0.3	0.0790	0.6940

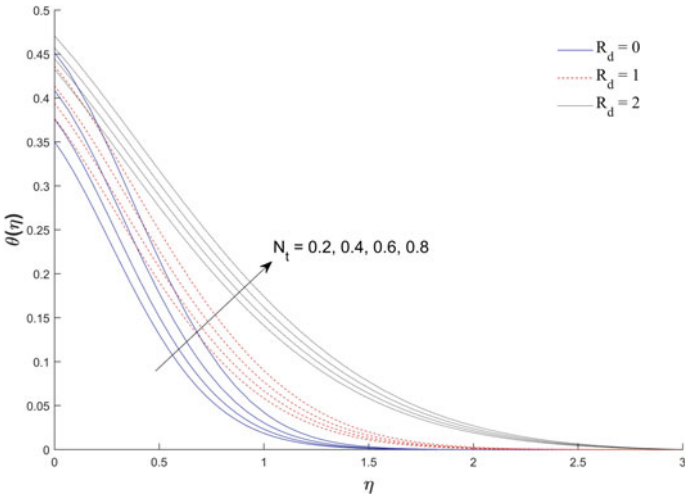

Fig. 2 Effect of N_t along with R_d on $\theta(\eta)$

temperature increases with the increase of both N_t and R_d whereas the nanoparticle concentration increases with N_t but decreases with an increase in radiation. Figure 4 describes the effect of N_t and R_d on the temperature derivative profile $(-\theta'(\eta))$ and it is clear that it increases with the increase of N_t and R_d. The results are important for calculating the Nusselt number since they have a direct relationship to its value when $\eta = 0$. The reason behind the fact is that the increase in N_t results the enhancement of thermophoresis forces which has the tendency to fast flow the nanoparticles from hot surface to cold surface away from stretching. This results in an increase of heat and mass transfer in the boundary layer region for nanoparticles.

Figures 5 and 6 illustrate how N_b affects the temperature and nanoparticle concentration profiles in conjunction with the specified radiation. The study elucidates that the temperature increases with the increment N_b but decreases with R_d whereas the concentration decreases with the increase in both N_b and R_d. The impact of N_b along with R_d on $-\theta'(\eta)$ is depicted in Fig. 7 and an increase is observed with the increase in N_b but an opposite trend is seen with R_d. It is well known that as Nb increases, so

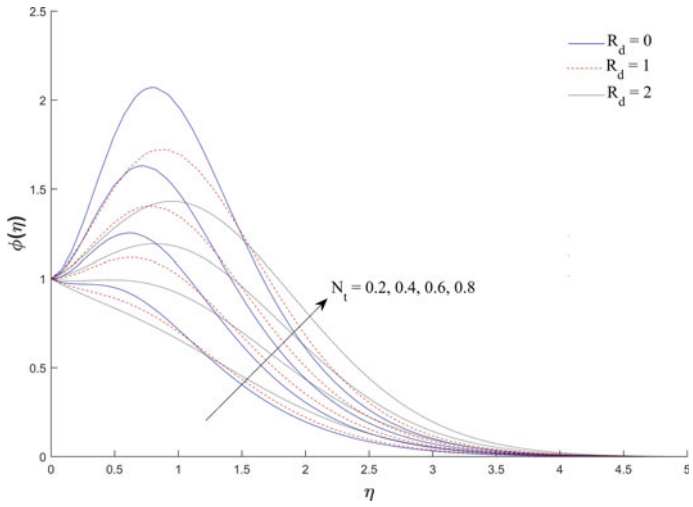

Fig. 3 Effect of N_t along with R_d on $\phi(\eta)$

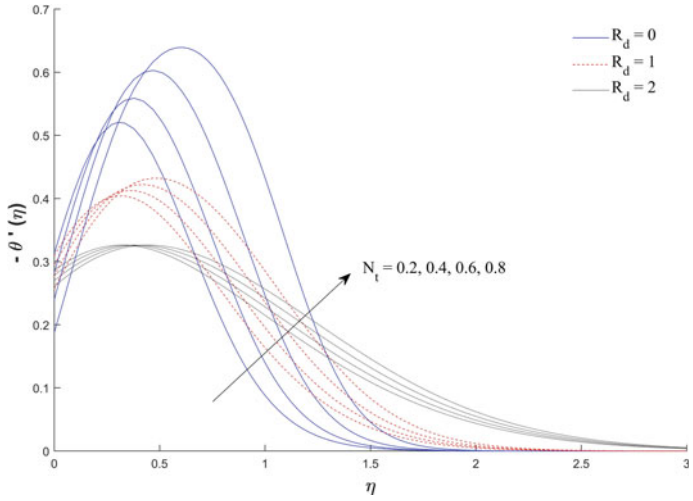

Fig. 4 Effect N_t of along with R_d on $-\theta'(\eta)$

does the random motion of nanoparticles, resulting in an increase in collisions with other nanoparticles. As a result, the kinetic energy is transformed into heat energy, and the temperature rises. But the rate of mass transfer decreases because of the tendency of the particle to get close to each other as Nb increases.

Figures 8 and 9 show the effect of Biot number γ on both temperature and nanoparticle concentration and it is observed that both increases with the increase in γ. The main reason behind the fact is that, increase in biot number means increase

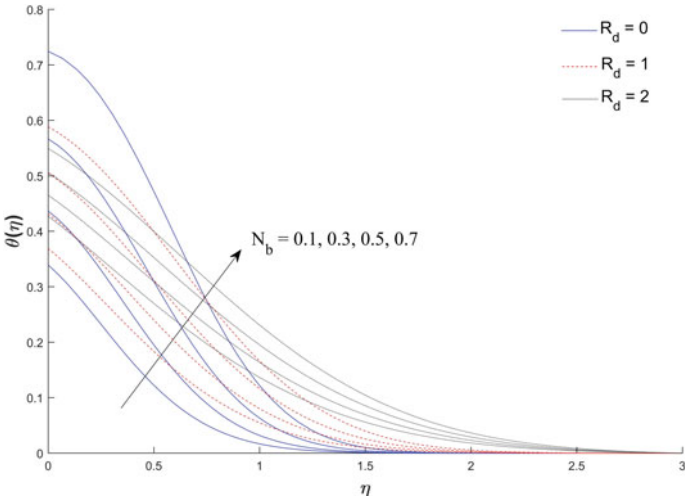

Fig. 5 Effect of N_b along with R_d on $\theta(\eta)$

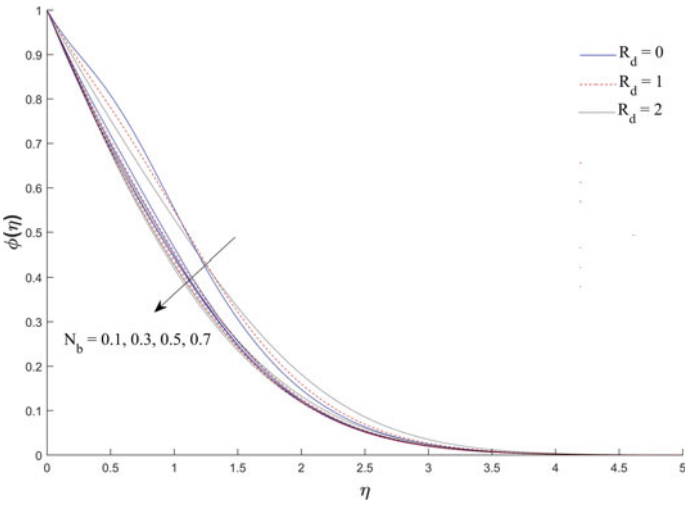

Fig. 6 Effect of N_b along with R_d on $\phi(\eta)$

in convective heat exchange at the surface which results in the increase in thermal boundary layer thickness and which in turn increases the nanoparticle concentration. Figures 10 shows that the temperature decreases with the increase of Prandtl number Pr whereas Fig. 11 shows that the nanoparticle concentration profile increases with Pr. The main reason behind the fact that with the higher value in Pr the heat diffuses

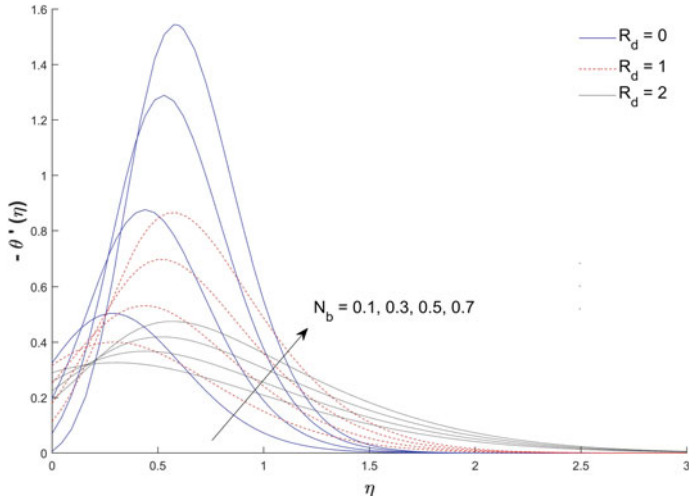

Fig. 7 Effect of N_b along with R_d on $-\theta'(\eta)$

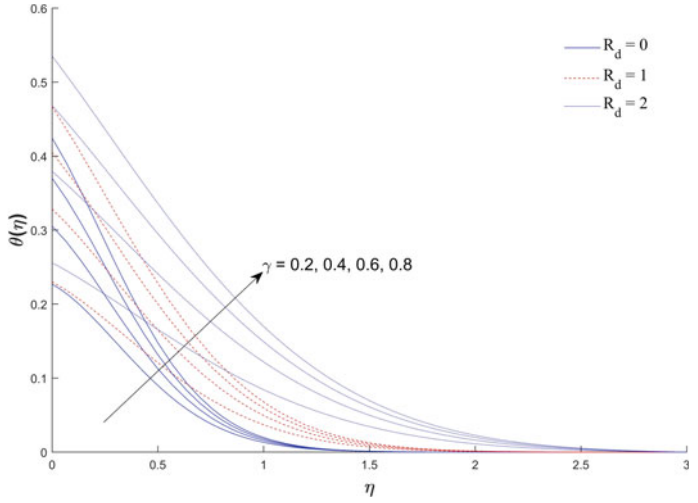

Fig. 8 Effect of γ along with R_d on $\theta(\eta)$

more rapidly than the momentum. It is also observed that at large Pr the temperature falls more drastically due to the fact that the large values of Pr leads to the low thermal conductivity.

Figure 12 depicts the impact of E_c on the temperature profile. We know that Eckert number expresses a direct relationship of flow's kinetic energy to the boundary layer enthalpy differences. This leads to the fact that the increases in E_c enhance the kinetic energy. Whereas it is well known that the temperature is an average kinetic energy.

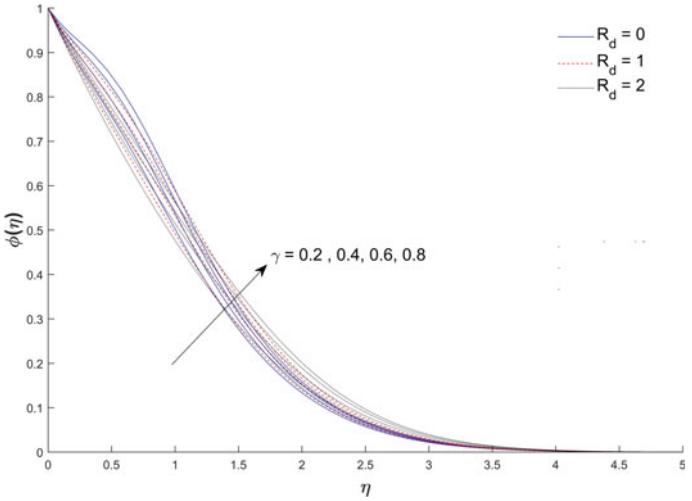

Fig. 9 Effect of γ along with R_d on $\phi(\eta)$

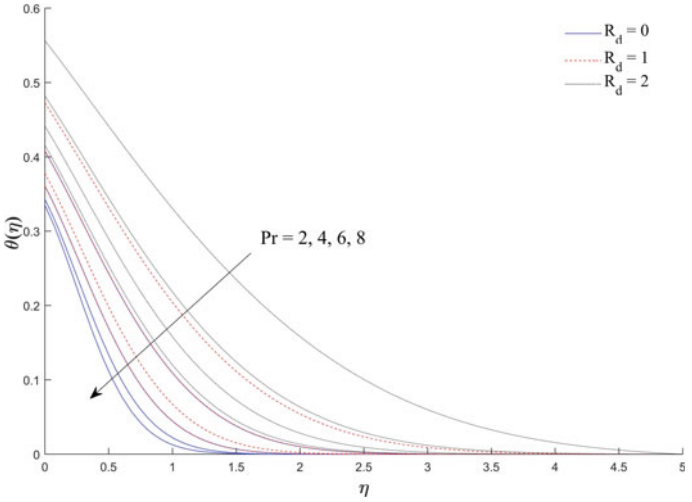

Fig. 10 Effect of Pr along with R_d on $\theta(\eta)$

Hence alternatively we can say that temperature rises with the increase in Eckert number and which can be clearly seen in the figure.

Figures 13 , 14 and 15 show the effect of magnetic parameters on velocity, temperature, and nanoparticle concentration respectively. It is noticed from the velocity profile that the velocity decreases with the increase in magnetic parameter. An exact opposite behavior is seen in the case of temperature profile where the temperature

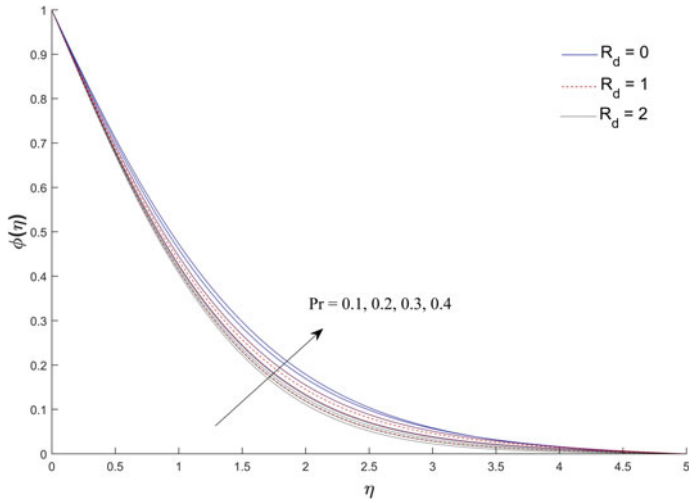

Fig. 11 Effect of Pr along with R_d on $\phi(\eta)$

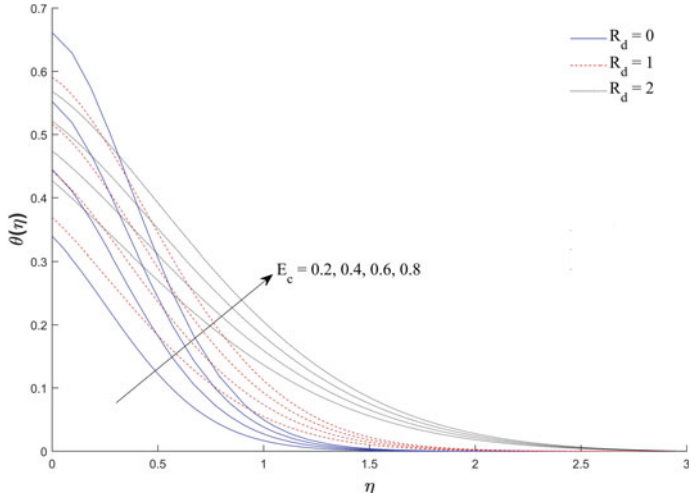

Fig. 12 Effect of E_c along with R_d on $\theta(\eta)$

increases with the increase in M and radiation R_d. In the case of nanoparticle concentration, it is clear from the graph that the concentration increases with the increasing magnetic parameter but decreases with stronger radiation. As the magnetic field parameter increases, a resistive force called a Lorentz force is produced which retards in the form magnetic pressure drop on the velocity, as a result the motion gets slowed down. Therefore the velocity decreases with the increasing value of M. Again due to the Lorentz force a resistance is offered to the flow which results in warming up

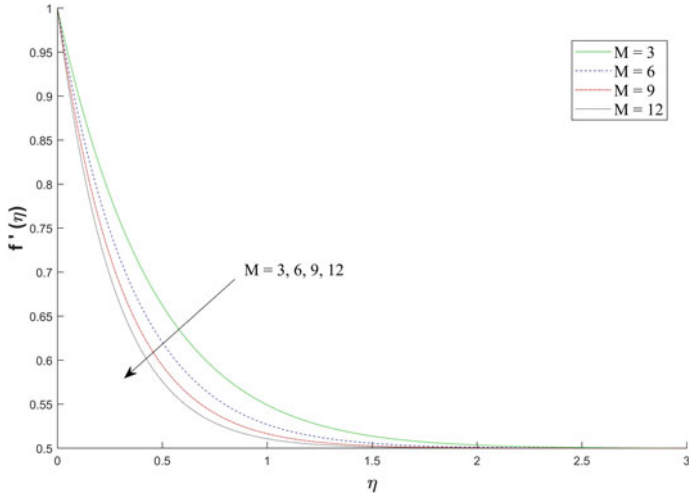

Fig. 13 Effect of M along with R_d on $f'(\eta)$

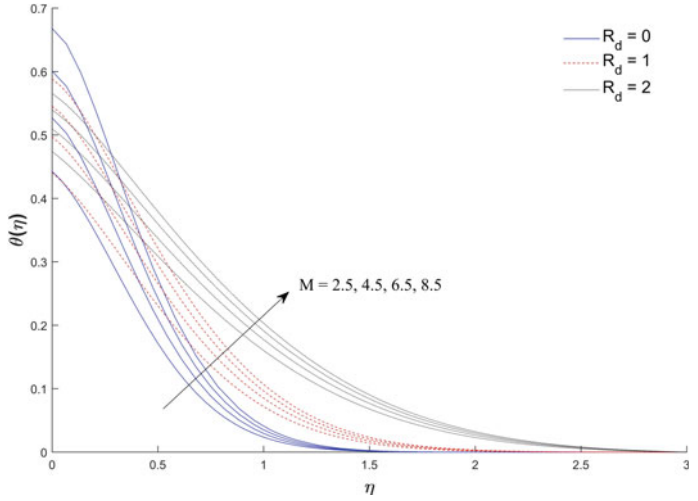

Fig. 14 Effect of M along with R_d on $\theta(\eta)$

the boundary layer region. Hence the temperature increases as the values of M gets increase.

The influence of Lewis number on temperature and nanoparticle concentration can be depicted in Figs. 16 and 17 respectively. It is noted that a growing behavior is found for temperature profile with the increment in Le and R_d whereas the concentration decreases with the increase in Le. It is observed that a smaller increase in Le results in larger differences in temperature and a thinner concentration boundary layer due to

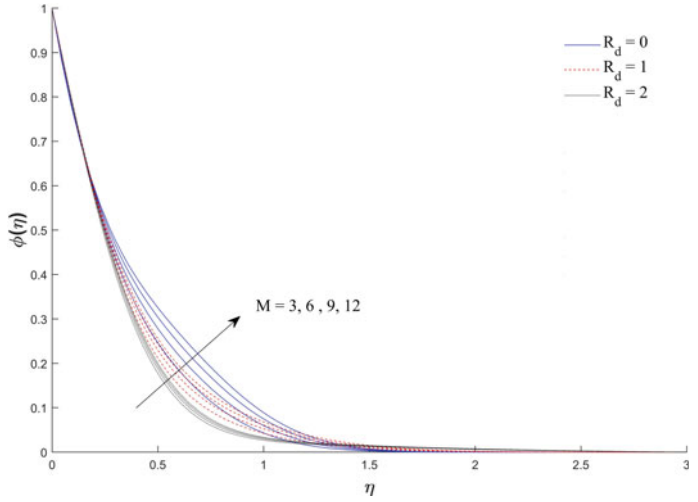

Fig. 15 Effect of M along with R_d on $\phi(\eta)$

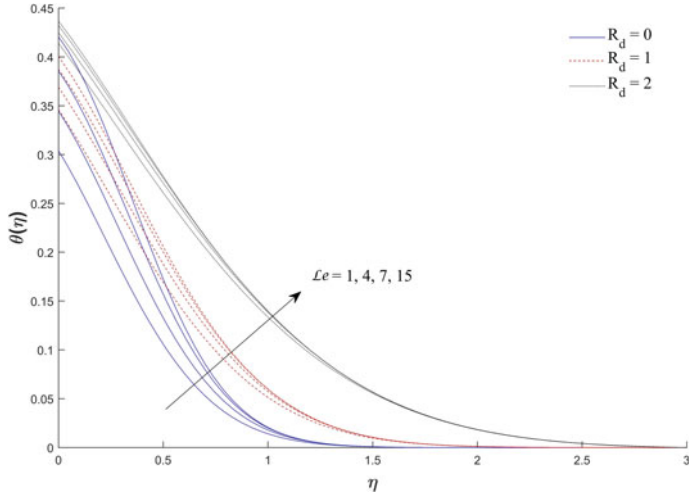

Fig. 16 Effect of Le along with R_d on $\theta(\eta)$

a weak molecular diffusivity. Figures 18 and 19 depicts the behavior of temperature profile for heat source parameter ($A > 0$) and heat sink parameter ($A < 0$) respectively. It is observed that the temperature of the thermal boundary layer increases with the increase in A (heat source parameter) and decreases with the decrease in A (heat sink parameter) under constant thermal radiation.

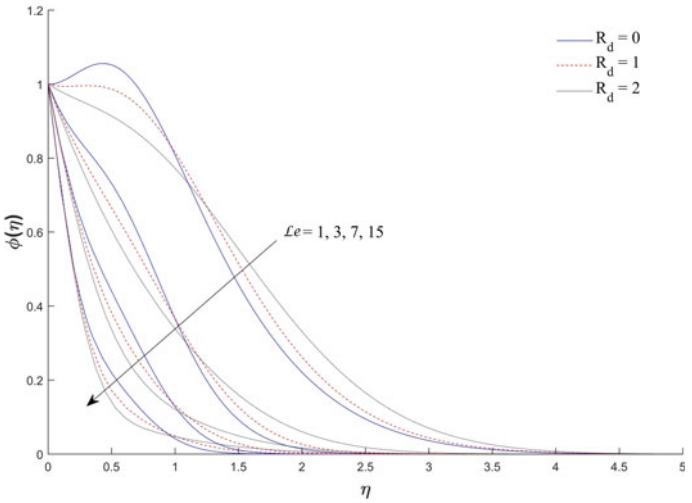

Fig. 17 Effect of Le along with R_d on $\phi(\eta)$

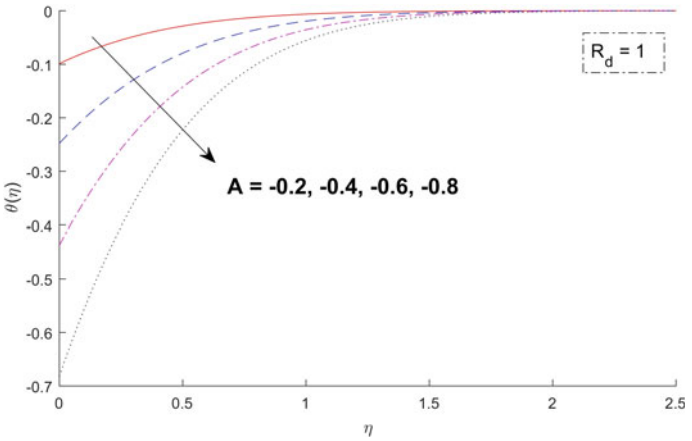

Fig. 18 Effect of $A < 0$ on $\theta(\eta)$

5 Conclusions

The influence of solar radiation on a constant two-dimensional MHD flow across a stretched plate is examined for various parameters in this study. The findings acquired in this investigation using the MATLAB programme bvp4c and the results obtained in the previous study utilizing the Runge Kutta Fourth Order Scheme showed great consistency. The impact of various parameters in our present investigation are as follows:

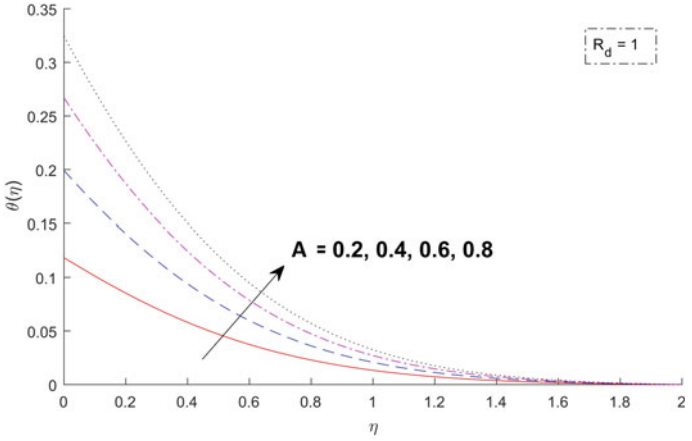

Fig. 19 Effect of $A > 0$ on $\theta(\eta)$

- The increasing value of Magnetic field parameter can decrease the nanoparticle velocity.
- The temperature distribution in the boundary layer region can be enhanced with the increment of Magnetic field parameter, Biot number Thermophoresis parameter, Brownian motion parameter, Heat source parameter, Lewis number and Eckert number.
- The temperature distribution diminishes with the increasing value of Prandtl number and Heat sink parameter.
- Nanoparticle volume fraction in the boundary layer region can be enriched by increasing the value of Thermophoresis parameter, Biot number, Magnetic field parameter, Lewis number and Prandtl number while it can decrease with the increase in Brownian motion parameter.
- The increasing value of Radiation parameter increases the Temperature profile and decreases the Nanoparticle volume fraction profile.
- The value of reduced Nusselt number is increased with the increase in Biot number and the Prandtl number and deceases with magnetic field parameter, Lewis number, Thermophoresis parameter and Brownian motion parameter.
- The value of reduced Sherwood number is increased with the increase in Brownian motion parameter, Magnetic field parameter, Prandtl number, Lewis number and Eckert number but decreases with Thermophoresis parameter and Biot number.
- It is very interesting to note that increase in Radiation parameter lead to the decrease in Reduced Nusselt number and increase in Reduced Sherwood number.
- The applicability of MATLAB's software bvp4c (Boundary layer problem of fourth-order) is ensured by verifying the findings as compared to the previously published results.
- The present study finds an application in efficient Solar collector, Cooling problems in industry, etc.

References

1. Akilu, S., Sharma, K. v., Baheta, A. T., & Mamat, R.: A review of thermophysical properties of water based composite nanofluids. In: Renewable and Sustainable Energy Reviews, vol. 66, pp. 654–678. Elsevier Ltd. (2016)
2. Bansal, J.L.: Magnetofluiddynamics of Viscous Fluids. Jaipur Publishing House, Jaipur India (1994)
3. Brewster, M.Q.: Thermal Radiative Transfer Properties. John Wiley and Sons, New York (1972)
4. Buongiorno, J.: Convective transport in nanofluids. J. Heat Transf. **128**(3), 240–250 (2006)
5. Choi, S.U.S.: Enhancing thermal conductivity of fluids with nanoparticles. ASME Int. Mech. Eng. Cong. Expo. **66**, 99–105 (1995)
6. Chutia, M., Deka, P.N.: Numerical study on MHD mixed convection flow in a vertical insulated square duct with strong transverse magnetic field. J. Appl. Fluid Mech. **8**(3), 473–481 (2015)
7. Eastman, J.A., Choi, S.U.S., Li, S., Yu, W., Thompson, L.J.: Anomalously increased effective thermal conductivities of ethylene glycol-based nanofluids containing copper nanoparticles. Appl. Phys. Lett. **78**(6), 718–720 (2001)
8. England, W.G., Emery, A.F.: Thermal radiation effects on the laminar free convection boundary layer of an absorbing gas. ASME J. Heat Transfer. **91**(1), 37–44 (1969)
9. Faizal, M., Saidur, R., Mekhilef, S., Alim, M.A.: Energy, economic and environmental analysis of metal oxides nanofluid for flat-plate solar collector. Energy Convers. Manage. **76**, 162–168 (2013)
10. Ghasemi, S.E., Hatami, M.: Solar radiation effects on MHD stagnation point flow and heat transfer of a nanofluid over a stretching sheet. Case Stud. Thermal Eng. **25** (2021)
11. Ghasemi, S.E., Hatami, M., Jing, D., Ganji, D.D.: Nanoparticles effects on MHD fluid flow over a stretching sheet with solar radiation: a numerical study. J. Mol. Liq. **219**, 890–896 (2016)
12. Gireesha, B.J., Mahanthesh, B., Shivakumara, I.S., Eshwarappa, K.M.: Melting heat transfer in boundary layer stagnation-point flow of nanofluid toward a stretching sheet with induced magnetic field. Eng. Sci. Technol. Int. J. **19**(1), 313–321 (2016)
13. Hayat, T., Imtiaz, M., Alsaedi, A., Kutbi, M.A.: MHD three-dimensional flow of nanofluid with velocity slip and nonlinear thermal radiation. J. Magn. Magn. Mater. **396**, 31–37 (2015)
14. Javadi, F. S., Saidur, R., Kamalisarvestani, M.: Investigating performance improvement of solar collectors by using nanofluids. In: Renewable and Sustainable Energy Reviews, vol. 28, pp. 232–245 (2013)
15. Khan, W.A., Makinde, O.D.: MHD nanofluid bioconvection due to gyrotactic microorganisms over a convectively heat stretching sheet. Int. J. Therm. Sci. **81**(1), 118–124 (2014)
16. Khan, W.A., Pop, I.: Boundary-layer flow of a nanofluid past a stretching sheet. Int. J. Heat Mass Transf. **53**(11–12), 2477–2483 (2010)
17. Kumar, M.A., Reddy, Y.D., Rao, V.S., Goud, B.S.: Thermal radiation impact on MHD heat transfer natural convective nano fluid flow over an impulsively started vertical plate. Case Stud. Thermal Eng. **24**, 100826 (2021)
18. Kuznetsov, A.V., Nield, D.A.: Natural convective boundary-layer flow of a nanofluid past a vertical plate. Int. J. Thermal Sci. **49**(2), 243–247 (2010)
19. Lee, S., Choi, -S, Li, S., Eastman, J.A.: Measuring Thermal Conductivity of Fluids Containing Oxide Nanoparticles (1999). http://heattransfer.asmedigitalcollection.asme.org/
20. Lenert, A., Nam, Y., Wang, N.E.: Heat transfer fluids. Ann. Rev. Heat Trans. **15**(2), 45 (2012)
21. Liu, Z.H., Hu, R.L., Lu, L., Zhao, F., Xiao, H.S.: Thermal performance of an open thermosyphon using nanofluid for evacuated tubular high temperature air solar collector. Energy Convers. Manage. **73**, 135–143 (2013)
22. Lv, Y.P., Shaheen, N., Ramzan, M., Mursaleen, M., Nisar, K.S., Malik, M.Y.: Chemical reaction and thermal radiation impact on a nanofluid flow in a rotating channel with Hall current. Sci. Rep. **11**(1) (2021)
23. Makinde, O.D., Aziz, A.: Boundary layer flow of a nanofluid past a stretching sheet with a convective boundary condition. Int. J. Therm. Sci. **50**(7), 1326–1332 (2011)

24. Mushtaq, A., Mustafa, M., Hayat, T., Alsaedi, A.: Nonlinear radiative heat transfer in the flow of nanofluid due to solar energy: a numerical study. J. Taiwan Inst. Chem. Eng. **45**(4), 1176–1183 (2014)
25. Otanicar, T.P., Phelan, P.E., Prasher, R.S., Rosengarten, G., Taylor, R.A.: Nanofluid-based direct absorption solar collector. J. Renew. Sustain. Energy **2**(3) (2010)
26. Pai, S.I.: Viscous Flow Theory: I Laminar Flow. D. VanNostrand Co., New York, USA (1956)
27. Patel, H.E., Sundararajan, T., Das, S.K.: An experimental investigation into the thermal conductivity enhancement in oxide and metallic nanofluids. J. Nanopart. Res. **12**(3), 1015–1031 (2010)
28. Rana, P., Bhargava, R.: Flow and heat transfer of a nanofluid over a nonlinearly stretching sheet: a numerical study. Commun. Nonlinear Sci. Numer. Simul. **17**(1), 212–226 (2012)
29. Raptis, A.: Radiation and free convection flow through a porous medium. Int. Commun. Heat Mass Transf. **25**, 289–295 (1998)
30. Rashidi, M.M., Vishnu Ganesh, N., Abdul Hakeem, A.K., Ganga, B.: Buoyancy effect on MHD flow of nanofluid over a stretching sheet in the presence of thermal radiation. J. Mol. Liq. **198**, 234–238 (2014)
31. Sarkar, A., Kundu, P.K.: Framing the upshot of Hall current on MHD unsteady nanofluid flow from a rotating spherical body in presence of solar radiation. Int. J. Ambient Energy (2021)
32. Schichting H.: Boundary Layer Theory, vol. 6. McGraw-Hill, New York (1964)
33. Shdaifat, M.Y.A., Zulkifli, R., Sopian, K., Salih, A. A.: Thermal and hydraulic performance of CuO/water nanofluids: a review. In: Micromachines, vol. 11, Issue 4 (2020)
34. Sparrow, E.M., Cess, R.D.: Radiation Heat Transfer. Hemisphere, Washington (1978)
35. Yousefi, T., Veysi, F., Shojaeizadeh, E., Zinadini, S.: An experimental investigation on the effect of Al_2O_3-H_2O nanofluid on the efficiency of flat-plate solar collectors. Renew. Energy **39**(1), 293–298 (2012)